Available online at www.sciencedirect.com
ScienceDirect
Journal of the European Ceramic Society 30 (2010) 2889–2896
www.elsevier.com/locate/jeurceramsoc

Fabrication and properties of ultra highly porous silicon carbide by the gelation–freezing method

Manabu Fukushima *, Masayuki Nakata, You Zhou, Tatsuki Ohji, Yu-ichi Yoshizawa

National Institute of Advanced Industrial Science and Technology (AIST), 2266-98 Shimo-Shidami, Moriyama-ku, Nagoya 463-8560, Aichi, Japan

Available online 18 April 2010

Abstract

Silicon carbide (SiC) with ultra high porosity and unidirectionally oriented micrometer-sized cylindrical pores was prepared using a novel gelation–freezing (GF) method. Gelatin, water and silicon carbide powder were mixed and cooled at 7 °C. The obtained gels were frozen from −10 to −70 °C, dried using a vacuum freeze drier, degreased at 600 °C and then sintered at 1800 °C for 2 h. The gels could be easily formed into various shapes, such as cylinders, large pipes and honeycombs using molds. Scanning electron microscopy (SEM) observations of the sintered bodies showed a microstructure composed of ordered micrometer-sized cylindrical cells with unidirectional orientation. The cell size ranging from 34 to 147 μm could be modulated by changing the freezing temperatures. The numbers of cells for the samples frozen at −10 and −70 °C were 47 and 900 cells/mm^2, respectively, as determined from cross-sections of the sintered bodies. The resulting porous SiC with a total porosity of 86%, exhibited air permeability from 2.3×10^{-11} to 1.0×10^{-10} m^2, which was the same as the calculated ideal permeability, and high compressive strength of 16.6 MPa. The porosity, number of cells, air permeability and strength of the present porous SiC were significantly higher than that reported for other porous SiC ceramics.
© 2010 Elsevier Ltd. All rights reserved.

Keywords: Shaping; Suspensions; Porosity; SiC; Membrane; Substrate; Structural applications

1. Introduction

Porous ceramics hold a significant position in industry for a variety of applications related with environmental protection and energy production. Those include filters and catalyst supports for environmental purification systems, thermal insulators for energy saving and solid oxide fuel cell (SOFC) supports for energy production. In these applications, shape forming is one of the most important factors. Advanced shaping technologies can facilitate porous ceramic components with complicated or large shapes, such as near-net shapes formed by gel casting or extrusion, and machined by cutting and polishing. In addition, porosity is another key factor, especially, where interconnected pores are required to provide high flux with low pressure drop in filter and catalyst supports. Thus, ultra highly porous components (porosity above 80%) with good permeability and desired shapes are essentially important in these industrial applications.

Among ceramic materials, silicon carbide (SiC) has attracted much attention due to its excellent thermal stability, mechanical properties and thermal shock resistance as well as corrosion resistance, which is due to its strong covalent bonding and low self-diffusion coefficient. Thus, SiC is a potential candidate material as filter and catalyst support for elevated temperature applications.

Over the past 5 years we have focused on the gelation–freezing (GF) method, which has advantages of high porosity (>70%), pore orientation control and near-net shape forming.[1–3] In the GF method, raw powder is firstly dispersed into water with a gelation agent. After gelation, the wet gel is immersed into cold ethanol, and ice crystals are formed, which results in the subsequent formation of pores. A vacuum freeze drier is used to dry the frozen gel, so that ice is sublimated without shrinkage of the green body. The green body is then sintered to obtain a porous ceramic. This process is available for near-net shaping, similar to the conventional gel casting method,[4] and is an environmentally friendly method because the pores are formed from ice crystals. In addition, the porosity is easily controlled by varying the solid load in the slurry.[3]

The preparation of porous ceramics by freeze casting route has recently been reported by many researchers. For examples, Deville et al.[5] synthesized porous alumina by controlling the freezing of ceramic slurries, and formed multilayered

* Corresponding author. Tel.: +81 52 736 7161; fax: +81 52 736 7405.
E-mail address: manabu-fukushima@aist.go.jp (M. Fukushima).

0955-2219/$ – see front matter © 2010 Elsevier Ltd. All rights reserved.
doi:10.1016/j.jeurceramsoc.2010.03.018

microstructures with homogeneous and well-defined architecture. Koh et al.[6,7] reported the fabrication of porous alumina (66–90%) with interconnected pore channels by the freezing of alumina/camphene slurries.

These previous studies indicate that the freezing conditions such as freezing temperatures and the additive to adjust the ice crystal formation have a significant effect on the properties and microstructure of the resulting porous ceramics. However, for the GF method, the relationship between the freezing conditions and the properties has not been systematically investigated. In this work, ultra highly porous SiC with various shapes was prepared by the GF method, where gelatin was used as a gelation agent. The use of gelatin in the GF process substantially facilitates near-net shape forming of gel casting and significantly raise porosity (since gelatin can retain a large amount of water), forming an oriented cylindrical ice crystal in the gelatin gel.

2. Experimental

2.1. Sample preparation

α-SiC (Fujimi Incorporated, Aichi, Japan) with an average particle size of 0.40 μm was used as a raw material. Al_2O_3 (Taimei Chemicals Co., Ltd., Japan) and Y_2O_3 (Shin-etsu Chemical Co., Ltd., Japan) were used as additives. Mixtures of additives/SiC of 4/96 with the additive of $Al_2O_3/Y_2O_3 = 6/4$ in weight ratio were blended in ethanol by ball milling. After drying of the slurry by evaporator and vacuum oven at 110 °C, the obtained powder was used for further processing.

The dried powder was mixed with a solution of gelatin (Wako Pure Chemical Industries Ltd., Tokyo, Japan) at around 50 °C. The mixing ratios of SiC powder/gelatin solution were 10/90 (v/v). The mixture was stirred using a planetary homogenizer (Thinky, type ARE-310, Tokyo, Japan). The slurry was put into the centrifuge container, which was revolved (800 rpm) while rotating (2000 rpm). The slurry was poured into a plastic mold and kept under ambient atmosphere to obtain a SiC powder dispersed gel. The plastic mold was then immersed into ethanol baths at various temperatures of −70, −40, −30, −20 and −10 °C. The gels were frozen in a manner similar to that previously reported.[1–3] The sublimation of ice crystals in the frozen gel was carried out under vacuum in a freeze drier at 10–35 °C for 24 h (Tokyo Rikakikai Co., Ltd., Model FDU-2100, Tokyo, Japan). Green bodies with ϕ70 mm and 10 mm thick were obtained, according to the shape of mold. Other shaped bodies, such as pipes or honeycombs, were also prepared by using various molds. The green bodies were degreased at 600 °C for 2 h and then sintered at 1800 °C for 2 h with a heating rate of 15 °C/min under an Ar gas flow.

2.2. Sample characterization

The porosity, microstructure, strength and permeability of the obtained specimens were characterized. Open porosity and bulk density were determined by the Archimedes method using water as an immersion medium, or the calculation of weight/dimension. The microstructures of fractured or polished surfaces were observed using scanning electron microscopy (JEOL, Model JSM-5600, Tokyo, Japan). The cell size and number of cells were measured using the intercept method or image analysis of the SEM micrographs. The compressive strength of samples with a diameter of ϕ17 mm and a height of 13 mm was measured using the universal testing machine (MTS Systems Corporation, Sintech 10/GL, Minnesota, USA) with a crosshead speed of 0.5 mm/min. Cylindrical specimens were loaded on the top and bottom surfaces. The load was parallel to the freezing direction. A minimum of five samples were tested to obtain the average strength.

The air permeability of the porous specimens was evaluated using Darcy's law:

$$\Delta P = \frac{\eta L Q}{\mu A} \quad (1)$$

where ΔP is the pressure drop from the entrance to exit of the sample, μ is the permeability, η is the dynamic viscosity of air, A is the cross-sectional area of the sample, L is the thickness of the sample, and Q is the flow rate of air through the sample. Samples cut into 3 mm in thickness (25 mm in a diameter) were fixed in a filter specimen holder (Advantec Toyo Kaisha Ltd., model LS-25) with an O-ring and a resin adhesive. The permeability was calculated from the slope of the line plotted for ΔP and Q using Eq. (1).

Further microstructural observations were carried out using X-ray computed tomography (CT; TDM1000-IS/SP, Yamato Scientific Co., Ltd., Tokyo, Japan). Three-dimensional (3D) images were constructed from micrographs using modeling software (VG-STUDIO, Nihon Visual Science Inc., Tokyo, Japan). Porosity distributions of the porous specimens were calculated using image analysis software (Multiscale modeler, JST-CREST project, Japan).

3. Results and discussion

Fig. 1 shows the photographs of the obtained porous SiC (A) cylinders, (B) large pipes, (C) honeycombs and (D) cut specimens (all of which were prepared using a freezing temperature of −40 °C). Various shaped molds were used to obtain gel bodies with the desired shape, similar to the traditional gel casting method for the fabrication of dense ceramics.[4] The cylindrical specimens (ϕ50 mm or ϕ25 mm) shown in Fig. 1(A) were formed using a ring-shaped mold. The large pipe (ϕ110 mm × 150 mm × 5 mm wall thickness) shown in Fig. 1(B) was shaped using a ring mold and core cylinder. Honeycomb specimens were prepared using a ring mold and 10 pins to generate non-through-holes. The porous specimens could be cut to varied sizes and shapes as shown in Fig. 1(D). Chipping was not observed during either wet or dry cutting processes. In addition, surface grinding and polishing to form flat surfaces were available for the specimens prepared by this GF method.

Fig. 2 shows the porosities of the porous SiC as a function of the freezing temperatures. It was found that the freezing temperature had almost no effect on the porosities. The densities of all specimens were around 14% (which means a total porosity of 86%), which was close to the solid load in the slurry (10%).

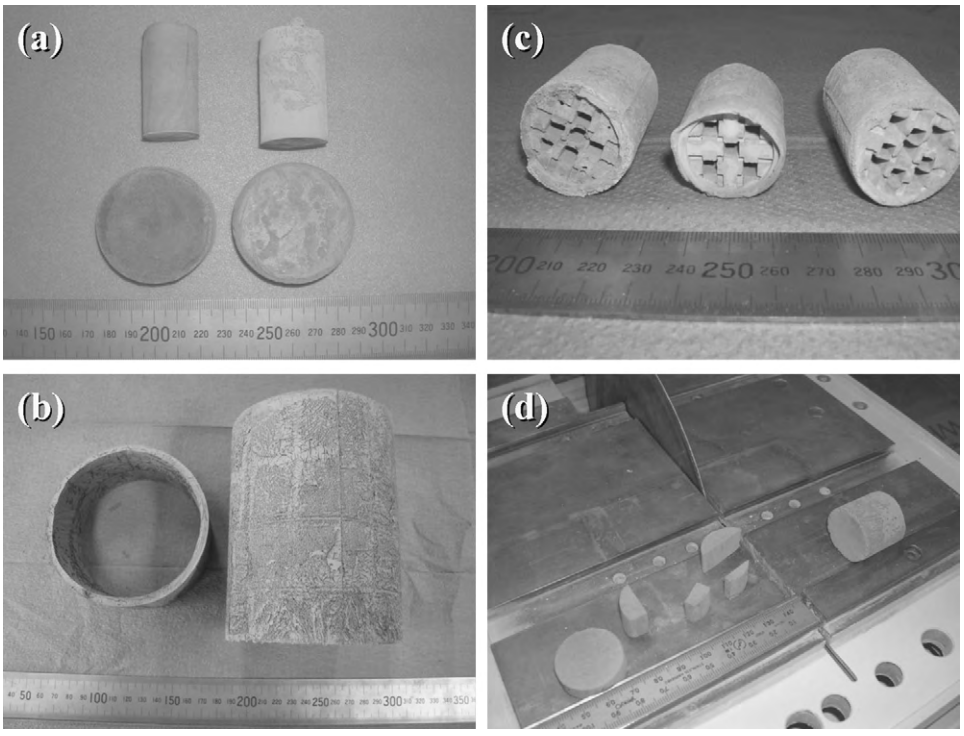

Fig. 1. Photographs of porous SiC obtained by freezing at −40 °C. (A) Cylindrical, (B) large pipe, (C) honeycomb, and (D) cut specimens.

On the other hand, closed porosities for all samples were less than 0.5%, which suggests that almost all water was completely converted to the interconnected pores.

Fig. 3 shows typical SEM micrographs of the porous SiC viewed in parallel (A and D) to the freezing direction as indicated by the arrows, and perpendicular (B and C; E and F) to freezing direction. The specimen shown in Fig. 3(A–C) was frozen at −10 °C and that shown in Fig. 3(D–F) was frozen at −70 °C. Specimens used with a dimension of around ϕ70 mm × 10 mm were firstly ground and polished to a thickness of 3 mm by removing the upper and the bottom ends, and the microstructures of the bottom side (the side in the ethanol bath) of the polished specimen were observed. In (A) and (D), highly oriented structures were found to form parallel to the freezing direction. These cylindrical pore structures are thought to be formed by the growing ice crystal. In addition, particles are rejected from the growing ice crystal and pushed aside during freezing. Connection points between cells (indicated by circles) were also observed where ice crystals were in contact. This unidirectional channeled structure is present within the entire sintered body of the porous body from the bottom toward the top, except the side and bottom surfaces. No dendritic structure due to ice crystal growth was observed, which is well-known in the freeze casting route of water or camphene based slurries (without an organic gelation agent).[6–10] In our preliminary experiments about normal freeze casting route, the side branching of dendritic ice crystal can be reduced by the addition of organic binder such as methylcellulose or gelatin (little to gelation). Thus, organic component is found to affect the ice crystal growth. In the present GF method, gelatin is thought to play a role of strongly preventing a side branching of dendritic ice crystal growth.

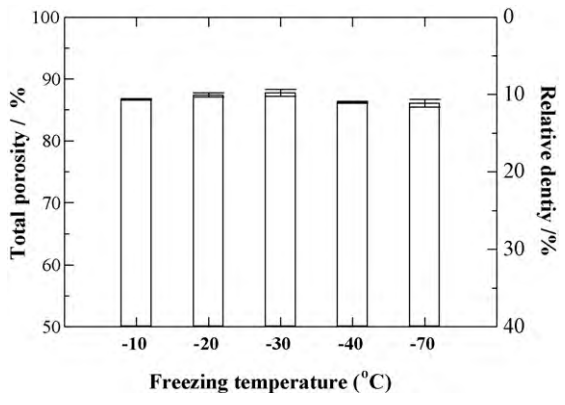

Fig. 2. Porosities of porous SiC obtained at various freezing temperatures.

Fig. 3(B and C) and (E and F) shows the cellular structure of pores, with a honeycomb-shape of micrometer-sized cells. This shape comes from the ice crystals, because polymeric additives except gelatin were not employed in the GF method. The cell shape was distinctly different from those found with foam, pore-forming agents and other freeze casting routes.[5–13] In especial, the microstructural features such as size and shape of cells and its distribution are highly homogeneous, compared to those of the specimens fabricated by other methods. The structure was observed throughout the porous body with the exception of the side and bottom surfaces, which were denser due to contact with the mold.

The freezing temperature was found to have a substantial effect on cell size. Comparison of Fig. 3(A and D) or (B and C) and (E and F) shows that the cell size and wall thickness of porous SiC frozen at −10 °C were significantly larger than those of SiC

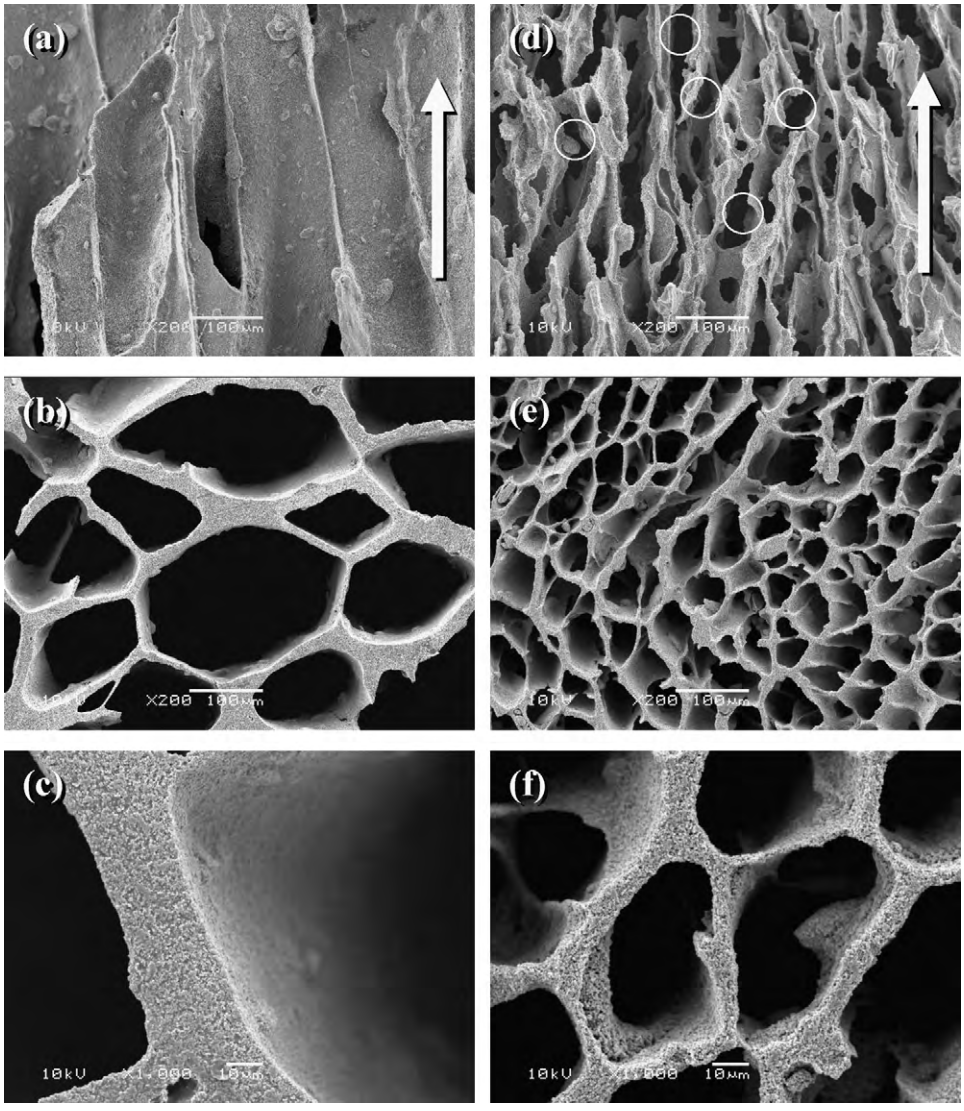

Fig. 3. SEM micrographs of porous SiC. Frozen at (A–C) −10 °C and (D–F) −70 °C, both parallel (A and D) and perpendicular (B and C; E and F) to the direction of freezing.

frozen at −70 °C. To clarify the effect of freezing temperature on the cell properties, the cell size and the number of cell are plotted as a function of freezing temperature in Fig. 4. The average cell sizes were 147, 62, 54, 40 and 34 μm, and the numbers of cells were 47, 262, 353, 612 and 900 cells/mm^2 for the specimens frozen at −10, −20, −30, −40, and −70 °C, respectively. The cell size decreased with the decrease in the freezing temperature, whereas the number of cell increased with the decrease in freezing temperature. The cell sizes were determined for the bottom side (in the direction of ethanol bath) of polished specimens. Those in the top surface (opposite to ethanol bath side) of the specimens used (3 mm thick) were around 10–15% larger than those of bottom side, which suggests that the formation temperature of ice crystals was somewhat different.

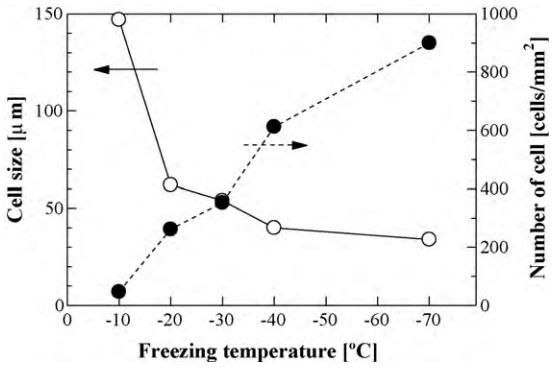

Fig. 4. Cell size and number of cell of porous SiC as a function of freezing temperature.

To further clarify the relationship between the freezing conditions and cell properties, the temperature of the gel body during freezing was measured. Fig. 5 shows a schematic illustration of the temperature measurement setup for a ϕ70 mm × 10 mm specimen and the measured temperature at the (a) surface, (b) center and (c) bottom of a gel body during freezing. In the temperature curve of −10 °C, all temperatures were raised up to −1 °C, about 7 min after the freezing starts. This phenomenon is well-known supercooling, in which the temperature increase

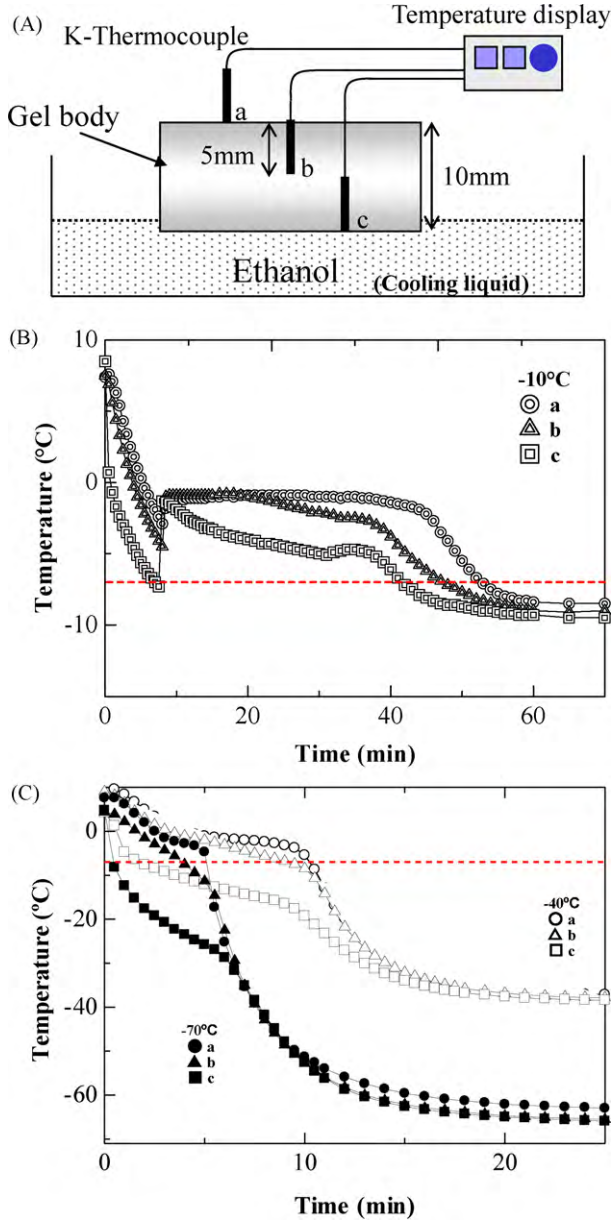

Fig. 5. (A) Schematic illustration of the temperature measurement and (B) the measured temperature of the gel body during freezing (a: surface, b: center and c: bottom).

is due to the release of latent heat during the conversion from water to ice. After that, the temperature curves were relatively flat from 7 to 40 min, suggesting the ongoing formation of ice crystals. This is due to the equilibrium between the release of latent heat (from water to ice) and heat flow into the ethanol bath. During this plateau stage, the temperature difference between measuring points a–c suggests that the formation temperature of ice crystals is different from the bottom of the gel to the top surface. The size of ice crystal formed at higher cooling temperature is generally larger than that formed at lower temperature. In fact, the cell size of the top surface side of the specimen was larger (ca. 10–15%) than that of the bottom side (ethanol bath side). At around 40 min, a temperature decrease at all measurement points was observed, which suggests that the formation of

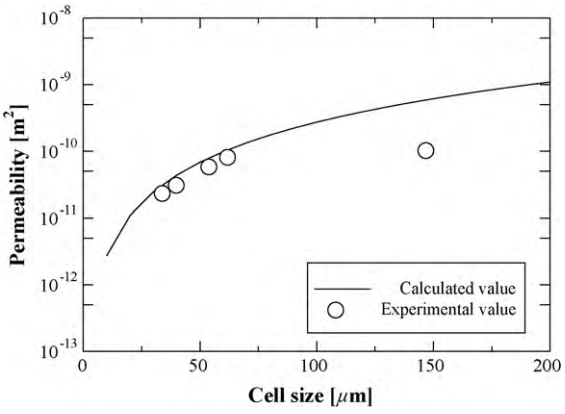

Fig. 6. Calculated and experimental air permeability as a function of cell size.

ice crystals was completed. The measured temperatures became almost the same (around −10 °C) after approximately 60 min.

On the other hand, in the plots of the specimens frozen at −40 and −70 °C, supercooling was not observed. This is due to the sufficiently lower cooling temperature. In addition, the plateau stages were very short compared with that for the specimen frozen at −10 °C, meaning that the formation of ice crystal is short time. Freezing at −40 °C resulted in gentle temperature curves during 0–10 min in (a) and (b) and during 0–9 min in (c), followed by the steep slopes to the set temperature of the ethanol bath. The curves of the gel frozen at −70 °C showed also relatively gentle slopes during the first 5–6 min, particularly (a) and (b), and then the temperatures steeply decreased to the set one.

According to the theory for the formation of ice crystals, the freezing temperature has a significant effect on the size of the ice crystals formed, especially in the temperature range from 0 to −7 °C, which is called as the zone of maximum ice crystal formation.[14] When the time required to pass this zone is short, the size of ice crystals formed can be reduced. From Fig. 5, the time to pass this zone became obviously short in the following order of bath temperature: −10 > −40 > −70 °C. The cell size of the sample frozen at −70 °C was smaller than those of the samples frozen at −10 and −40 °C (Fig. 5), which suggests that the size of the ice crystals formed was reduced by lowering of the freezing temperature.

In addition to the variation in cell size by the freezing temperature, the connectivity among the cells was investigated by air permeability measurements. Fig. 6 shows the relationship between cell size and permeability, and the calculated ideal permeability for comparison. The gas flow is parallel to the freezing direction. The calculated permeability is shown assuming an ideal model of capillary permeability, where unidirectional capillary tubes are aligned in parallel to the gas flow direction (through-holes from gas influx to efflux port). The ideal permeability (μ) is calculated according to the following equation:

$$\mu = \frac{d^2 \times P}{32} \quad (2)$$

where d and P indicate the diameter of capillary and porosity (volume ratio of capillary), respectively.[15] In this calculation,

permeability was plotted using the average porosity of the specimens (86%) and continuously varied pore size. The calculated permeability indicated a gradual increase with increased cell size according to the parabolic law. Then, seen from the experimental values, the permeations of porous SiC were 2.27×10^{-11}, 3.02×10^{-11}, 5.67×10^{-11}, 7.92×10^{-11} and 1.04×10^{-10} m^2 for the specimens frozen at −70, −40, −30, −20 and −10 °C, respectively. These were in good agreement with the calculated values, except that of the specimen frozen at −10 °C (cell size 147 μm). The experimental permeability of the specimen frozen at −10 °C was around 0.16 times lower than that of the ideal model. This difference may be attributed to discontinuous connectivity between cells. The cells were not completely straight, but some were bent by the contact points between ice crystals. In fact, some contact points were observed in the specimen frozen at −70 °C (Fig. 3(D)), whereas no significant contact points were found in the specimen frozen at −10 °C. In such a case, resistance to fluid flow increases, which results in lowering of the permeability. On the other hand, these permeabilities were just observed in the parallel to the freezing direction. The permeability in perpendicular to the freezing direction has not been measured, but that must be lower due to the insufficient connectivity between cells.

Compared to the air permeability of other porous ceramics with similar cell size, Isobe et al. reported that porous alumina with 39% porosity and pore sizes around 40 μm had permeability of 3.9×10^{-13} m^2.[16] Tomita et al. reported that porous silica foam with 81% porosity and cell sizes around 150 μm had permeability of 9.4×10^{-11} m^2.[17] The permeabilities obtained in the present study were substantially higher than those of the previous studies, and were also higher than that required for a commercially available diesel particulate filter (DPF) (10^{-11} to 10^{-12} m^2).[17] In contrast, the gas permeability of ceramic foam prepared by the sponge method was reported to be much higher at around 10^{-7} m^2,[18] although the pore size of the foam was much larger (around submillimeter) than that of the present specimens. The permeability of foam with similar pore size and porosity was approximately 10^{-11} to 10^{-10} m^2; therefore, the air permeability of porous ceramic prepared by the GF method can be concluded to be high, due to the sufficient connections between cells formed by the contact of ice crystals during freezing.

In order to understand the internal microstructure of porous SiC, X-ray CT scans and image analyses were conducted. Fig. 7(A) shows a typical specimen used (micrographs were observed for the center part of the specimen: around ϕ1.3 mm × 0.4 mm), (B) a typical micrograph of a specimen frozen at −10 °C (measured per 1.5 μm), (C and D) 3D images constructed from micrographs (specimens frozen at −10 and −70 °C, respectively), and (E) the cell area ratio of porous SiC (frozen at −10 and −70 °C). The micrograph showed a similar cellular structure to that obtained from SEM observations. In the 3D images, the cells are shown to be of uniform size and highly interconnected with unidirectional orientation, which are highly homogeneous than those of the specimens prepared by other methods. In Fig. 7(E), all micrographs (ca. 320 micrographs) were firstly converted to black-and-white images, and then the cell area ratios (as porosity) were calculated for each micrograph and plotted. The results show a cell/wall area ratio of approximately 85–86%, which is consistent with the porosity measured by Archimedes method. Furthermore, almost constant values were obtained in the measurement part, which suggests that the porosity was constant even at the micrometer level. Therefore, the GF method can provide constant porosity and uniform porosity distribution.

Table 1
Typical properties of porous SiC.

Properties	Freezing temperature	
	−10 °C	−70 °C
Open porosity	86.8%	86.5%
Closed porosity	0.1%	0.4%
Cell size	147 μm	34 μm
Cell thickness	20 μm	6 μm
Number of cell	47 cells/mm^2	900 cells/mm^2
Compressive strength	5.2 ± 0.8 MPa	16.6 ± 1.4 MPa
Permeability	1.04×10^{-10} m^2	2.27×10^{-11} m^2

Typical properties of highly porous SiC are summarized as follows. Cell wall thickness of porous SiC showed 20 and 6 μm. That was much smaller than that of commercially available DPF and catalyst support prepared by extrusion. In such applications, high porosity and thin wall thickness are desired, because of low pressure drop. This GF method is expected to be a promising process for filter and support applications. Then, compressive strength showed 5.2 and 16.6 MPa, where load was parallel to the cell (freezing direction). Strength increased with decreased cell size. This tendency has been observed in many other porous ceramics and is attributed to a larger defect size. Typical compressive strengths of the porous SiC prepared by other methods were ∼10 MPa with porosity of ∼70% and cell size of 20 μm and 16.7 MPa with porosity of 80% and cell size of 20–100 μm, which had similar cell size and porosity to the present porous SiC.[19–21] The strength of the present porous SiC was found to be similar or higher than that obtained by other methods, regardless of higher porosity. This comes from the packing of particles. Previous works on freeze casting suggested that the raw powder was highly packed upon freezing.[11] During freezing, the particles in the gel are concentrated by the separation of water and the following formation of ice crystals. Then, the particles are thought to be pressed by the volume increase from water to ice, as observed by the packing of particles in the cell walls (Fig. 3(C) and (F)). On the other hand, the anisotropy of compressive strength has not been investigated. For the present measurements, load was parallel to the freezing direction. Seen from the previous report, the compressive strength in perpendicular to the cell seems to be lower values in porous cellular ceramics (Table 1).[22]

These obtained results suggest that the freezing condition can be key factor to control the cell size, the number of cell, the permeability and the strength. The present porous SiC prepared by GF method showed high porosity, high strength and high permeability, compared to the properties of the porous SiC prepared by other methods. The GF method is expected to be a promising process for many applications.

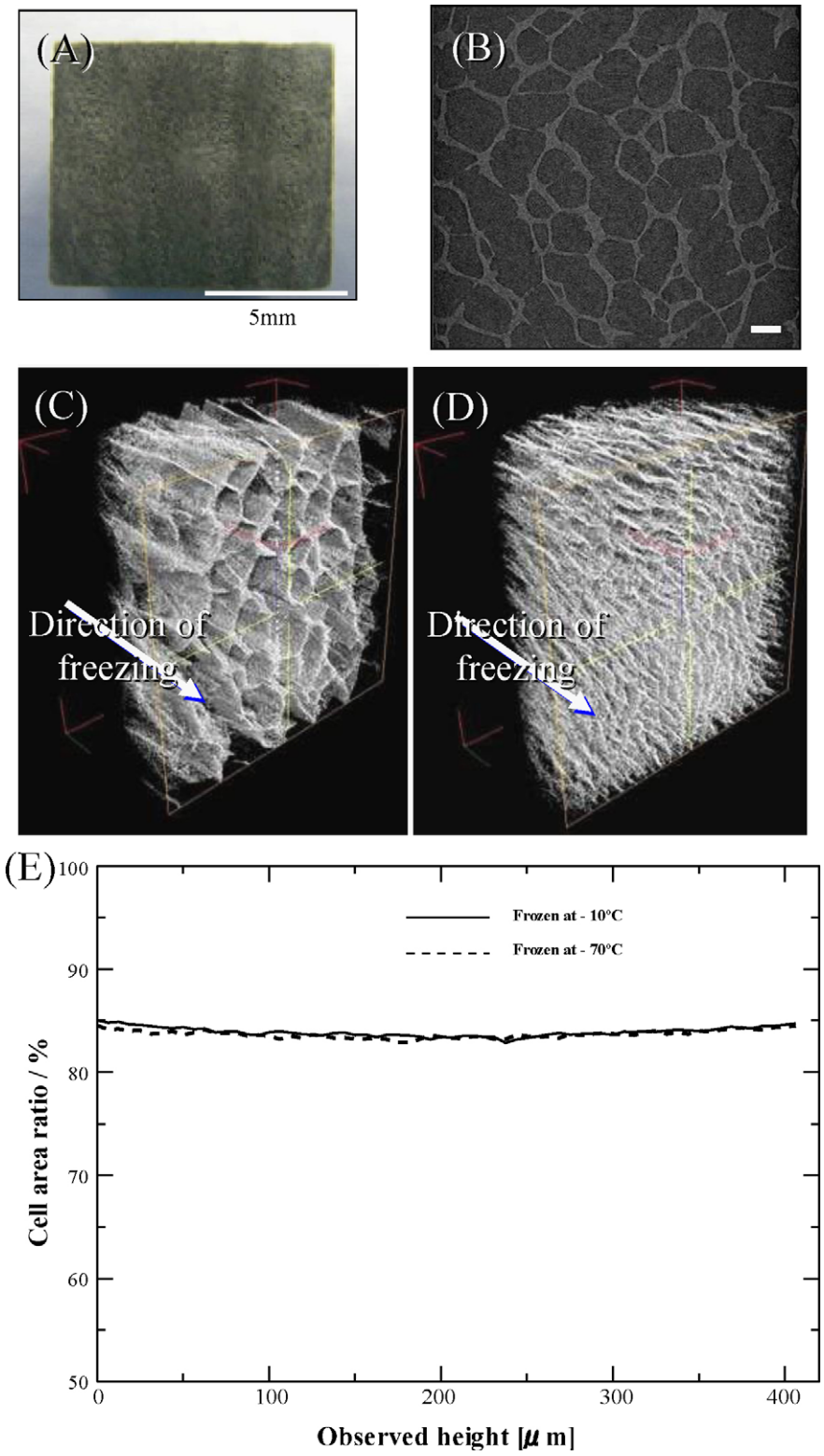

Fig. 7. (A) Photograph of a typical specimen. (B) Micrograph of specimen frozen at −10 °C (scale bar: 100 μm). (C and D) 3D images constructed from micrographs (specimens frozen at −10 and −70 °C, respectively). (E) Cell area ratio of porous SiC (specimens frozen at −10 and −70 °C, respectively).

4. Conclusions

SiC with ultra high porosity around 86% was prepared through a novel GF method using gelatin solution as a gelation agent at various freezing concentrations. This unique technique can be used to provide various shaped components by use of specific molds, and has the same advantages of the traditional gel casting method. Cylindrical shaped cells form interconnected, oriented, micrometer-sized pores, due to the formation of ice crystals during freezing. The cell size could be controlled

within the range of 34–147 μm by varying the freezing temperature. The average number of cell was in the range from 47 to 900 cells/mm^2. The resulting porous SiC exhibited high air permeability of 2.3×10^{-11} to 1.0×10^{-10} m^2, which was almost similar to ideal gas permeation, and high compressive strength of 16.6 MPa. This novel fabrication method is a potential process applicable for the production of various porous components such as filters and supports.

References

1. Nakata M, Tanihata K, Yamaguchi S, Suganuma K. *J Ceram Soc Jpn* 2005;**113**:712–5.
2. Nakata M, Fukushima M, Yoshizawa Y. *Ceram Eng Sci Proc* 2008;**28**(7):139–44.
3. Fukushima M, Nakata M, Yoshizawa Y. *J Ceram Soc Jpn* 2008;**116**:1322–5.
4. Young AC, Omatete OO, Janney MA, Menchhofer PA. *J Am Ceram Soc* 1991;**74**:612–8.
5. Deville S, Saiz E, Tomsia AP. *Acta Mater* 2007;**55**:1965–74.
6. Koh Y-H, Song J-H, Lee E-J, Kim H-E. *J Am Ceram Soc* 2006;**89**:3089–93.
7. Yoon B-H, Lee E-J, Kim H-E, Koh Y-H. *J Am Ceram Soc* 2007;**90**: 1753–9.
8. Ding S, Zeng Y-P, Jiang D. *J Am Ceram Soc* 2007;**90**:2276–9.
9. Fukasawa T, Deng ZY, Ando M, Ohji T, Kanzaki S. *J Am Ceram Soc* 2001;**84**:230–2.
10. Fukasawa T, Deng ZY, Ando M, Ohji T, Kanzaki S. *J Am Ceram Soc* 2002;**85**:2151–5.
11. Araki K, Halloran JW. *J Am Ceram Soc* 2005;**88**:1108–14.
12. Colombo P. *J Eur Ceram Soc* 2008;**28**:1389–95.
13. Chen C-H, Takita K, Ishiguro S, Honda S, Awaji H. *J Eur Ceram Soc* 2005;**25**:3257–64.
14. Tsuyuki H. *Shokuhin kakou-gaku*. Kyoritsu Shuppan; 2007. pp. 14–16 (in Japanese).
15. Tomita T, Kawasaki S, Okada K. *J Porous Mater* 2005;**12**:123–9.
16. Isobe T, Kameshima Y, Nakajima A, Okada K, Hotta Y. *J Eur Ceram Soc* 2007;**27**:53–9.
17. Tomita T, Kawasaki S, Okada K. *J Porous Mater* 2004;**11**:107–15.
18. Innocentini MDM, Salvini VR, Pandolfelli VC, Coury JR. *Am Ceram Soc Bull* 1999;**82**:78–84.
19. Eom J-H, Kim Y-W, Song I-H, Kim H-D. *J Eur Ceram Soc* 2008;**28**:1029–35.
20. Kim Y-W, Eom J-H, Wang C, Park CB. *J Am Ceram Soc* 2008;**91**:1361–4.
21. Ganesh I, Jana DC, Shaik S, Thiyagarajan N. *J Am Ceram Soc* 2006;**89**:3056–64.
22. Esposito L, Sciti D, Piancastelli A, Bellosi A. *J Eur Ceram Soc* 2004;**24**:533–40.